

Global degradation kinetics of pine needles in air

M.J. Safi, I.M. Mishra*, B. Prasad

Department of Chemical Engineering, Indian Institute of Technology, Roorkee 247 667, India

Received 27 June 2002; received in revised form 23 September 2003; accepted 23 September 2003

Abstract

Pine needles are available in large quantities in the hilly region of Himalayas in India. Pine needles have good energy potential for exploitation through pyrolysis and gasification. This paper deals with the thermal degradation characteristics of pine needles and its kinetics. Thermal degradation analysis has been done by using a thermogravimetric analyzer from room temperature to 900 °C in air atmosphere at different heating rates, viz. 5, 10, 15, 25 and 30 K min⁻¹. The TGA, DTG and DTA curves exhibited four distinct degradation zones. However, at the low heating rate of 5 K min⁻¹, only three degradation zones were found. The second, third and fourth zones had higher values of activation energy than the first zone. The kinetic parameters were determined by using several methods proposed in the literature assuming single step, irreversible reaction for a particular zone. Agrawal and Sivasubramanian [AIChE J. 33 (1987) 6] method was found to be most consistent. For the total degradation zone the orders of reaction were found in the range of 0.00–2.50 by using Agrawal and Sivasubramanian [AIChE J. 33 (1987) 6] approximation, the activation energy in the range of 34.60–85.34 kJ mol⁻¹ and the preexponential factor in the range of 3.29×10^4 to 5.98×10^6 mg¹⁻ⁿ min⁻¹. The relative simplicity of the model gives it the potential for applications in the design of large scale biomass-pyrolysis facility in remote areas.

© 2003 Elsevier B.V. All rights reserved.

Keywords: Oxidative degradation; Kinetics; Biomass; Pine needles; DTA; TGA

1. Introduction

Pine needles are abundantly available in the hilly region of the Himalayas in the Indian subcontinent. The lower heating value of the pine needles is found to be in the range of 18.0–20.00 MJ kg⁻¹ [1,2]. The heating value of pine needles is comparable to that of saw dust (18.2 MJ kg⁻¹) and fuel oil (~18.75 MJ kg⁻¹) and more than that of wood (15.82 MJ kg⁻¹) [1–3]. Table 1 presents the proximate and ultimate analysis of pine needles along with those of rice hulls, saw dust, village rice husk, pressmud and bagasse as reported by different investigators. From Table 1, it is clear that pine needles have higher fixed carbon and lower ash content than rice husk, rice hulls and saw dust; comparable volatile content with that of saw dust. The proximate and ultimate analysis of pine needles as shown in Table 1 and the energy content of pine needles indicate that pine needles are a good source to meet energy demands of the hilly region of Himalayas. On thermal decomposition, pine needles gener-

ate flammable gases such as light volatiles, carbon monoxide, hydrogen with other organic vapors. Through pyrolysis, pine needles can be densified in the form of briquettes which may be used as a smokeless fuel and can also be used to generate electric power through gasification process. Thermal gasification of biomass provides an excellent solution to the problem of energy recovery and waste disposal. It provides: (i) clean fuel, (ii) higher heating value per unit mass, (iii) higher combustion efficiency, and (iv) environmentally friendly technology. Since pine needles pose serious threat to forests from fires, their collection and disposal for energy recovery is a very attractive proposition.

Gasification of organic materials such as pine needles produces a mixture of gases under carefully controlled temperature, pressure and atmospheric conditions in a gasifier in the presence of an oxidizing agent like air or oxygen. Compared with oxygen, air gasification lowers the heating value of the gas due to nitrogen dilution of the gases. The understanding of the chemical kinetics of the oxidative and thermal degradation of pine needles represents a crucial phase in the proper design of the energy conversion and gasification systems. This has motivated a number of experimental investigations usually based on thermogravimetric analysis

* Corresponding author. Tel.: +91-1332-285720; fax: +91-1332-273560.

E-mail address: imishfch@iitr.ernet.in (I.M. Mishra).

Table 1
Proximate and ultimate analyses of pine needles and other biomass

| Investigator | Type of biomass | Volatile matter | Fixed carbon | Ash | Lower heating value | |
|---|-------------------|-----------------|--------------|----------|------------------------|-------|
| (a) Proximate analysis (% dry basis) and lower heating value (MJ kg ⁻¹) | | | | | | |
| Iyer et al. [2] | Pine Needles | 72.40 | 26.10 | 1.50 | 16.7 | |
| Safi [1] | Pine Needles | 74.19 | 24.07 | 1.74 | 18.5 | |
| Gangavati [3] | Saw dust | 76.00 | 20.40 | 3.60 | 15.66 | |
| Gangavati [3] | Village rice husk | 66.20 | 13.80 | 20.00 | 12.84 | |
| Gangavati [3] | Rice hulls | 66.10 | 14.70 | 19.20 | 13.67 | |
| Gangavati [3] | Pressmud | 54.00 | 26.00 | 20.00 | 11.98 | |
| Gangavati [3] | Bagasse | 53.90 | 35.00 | 11.10 | 15.12 | |
| Investigator | Type of biomass | Carbon | Hydrogen | Nitrogen | Oxygen (by difference) | Ash |
| (b) Ultimate analysis (%) | | | | | | |
| Prasad and Kuester [16] | Saw dust | 47.36 | 5.30 | 0.04 | 46.76 | 0.50 |
| Gangavati [3] | Saw dust | 43.94 | 6.18 | 0.61 | 45.67 | 3.60 |
| Gangavati [3] | Village rice husk | 37.43 | 6.01 | 1.32 | 35.24 | 20.0 |
| Gangavati [3] | Rice hulls | 37.40 | 5.54 | 0.34 | 37.52 | 19.20 |
| Gangavati [3] | Pressmud | 44.50 | 5.60 | 1.10 | 28.80 | 20.00 |
| Gangavati [3] | Bagasse | 44.10 | 5.26 | 1.00 | 38.54 | 11.10 |
| Safi [1] | Pine needles | 45.81 | 5.38 | 0.98 | 46.11 | 1.72 |

under oxidizing environments, simulating the temperature and oxygen concentration conditions of combustors/gasifiers [4]. No study has reported the thermal degradation characteristics and kinetics of pine needles under oxidizing environment.

2. Materials and methods

Pine needle samples were collected from the underneath of the pine avenue in the IIT, Roorkee campus. About 20 kg of pine needles were brought to the Department of Chemical Engineering and were sun dried. Dried material was stored in a polyethylene bag for future use. For the physico-chemical and thermal characterization of pine needles, a sample of approximately 1 kg of pine needles was further oven-dried at 105 °C for 2 h and ground in a laboratory ball mill. The ground matter was further classified by using two IS sieves of mesh size 180 and 600 μm . The sieved powdery sample having size distribution between 180 and 600 μm was stored in airtight plastic containers for future use. The proximate analysis of sieved pine needles sample was carried out as per procedure laid in the Bureau of Indian Standards code IS: 1350 (PART 1)-1984. The bulk density of the sample was determined by using a bulk density apparatus (Micro Scientific Works, Delhi).

A Stanton Redcroft Model STA-781 thermogravimetric analyzer was used in the present study to continuously monitor weight changes in pine needles sample due to drying, volatilization, and gasification as the sample followed a linear heating program. The instrument also provided the continuous recording of the DTG and DTA curves, in terms of wt.% loss per minute and temperature difference in mV (for DTA) which could be converted as per calibration chart to obtain temperature difference between the alumina sample

and the pine needle sample at any temperature under temperature programmed heating (from 0 to 30 K min⁻¹).

The principal experimental variables which could affect the thermal degradation characteristics in a TGA are the pressure, the purge gas flow rate, the heating rate, the weight of the sample and the sample size fraction. In the present study, the operating pressure was kept slightly positive, the purge gas (air) flow rate was maintained at 50 ml min⁻¹ and the heating rate was varied from 5 to 30 K min⁻¹. The uniformity of the sample was maintained by using a 10 mg sample and spreading it uniformly over the crucible base in all the experiments. The details of the experimental conditions, equipment and thermochemical–chemical properties of pine needles are presented elsewhere [1].

3. Results and discussion

The TGA, DTG and DTA curves for the 5, 15 and 30 K min⁻¹ heating rates are shown in Figs. 1–3, respectively. The curves for 10 and 25 K min⁻¹ heating rates are not shown here. Figs. 1–3 show the trend of the curves with increasing heating rates. The TGA curves show that there is an initial loss of moisture from the samples starting at around 27–50 °C and continuing up to about 180 °C. As the heating rate increases the drying temperature zone also increases. Higher temperature drying (>100 °C) occurs due to the loss of surface tension bound water of the ground sample particles. The nature of a TGA curve in combination with the corresponding DTG peaks gives a clear indication of the number of stages of the thermal degradation. During thermal degradation in air, weight loss occurs continuously until the weight becomes almost constant. The distribution of volatiles released during thermal degradation is shown in Table 2. TGA and DTA curves were used to deduce drying

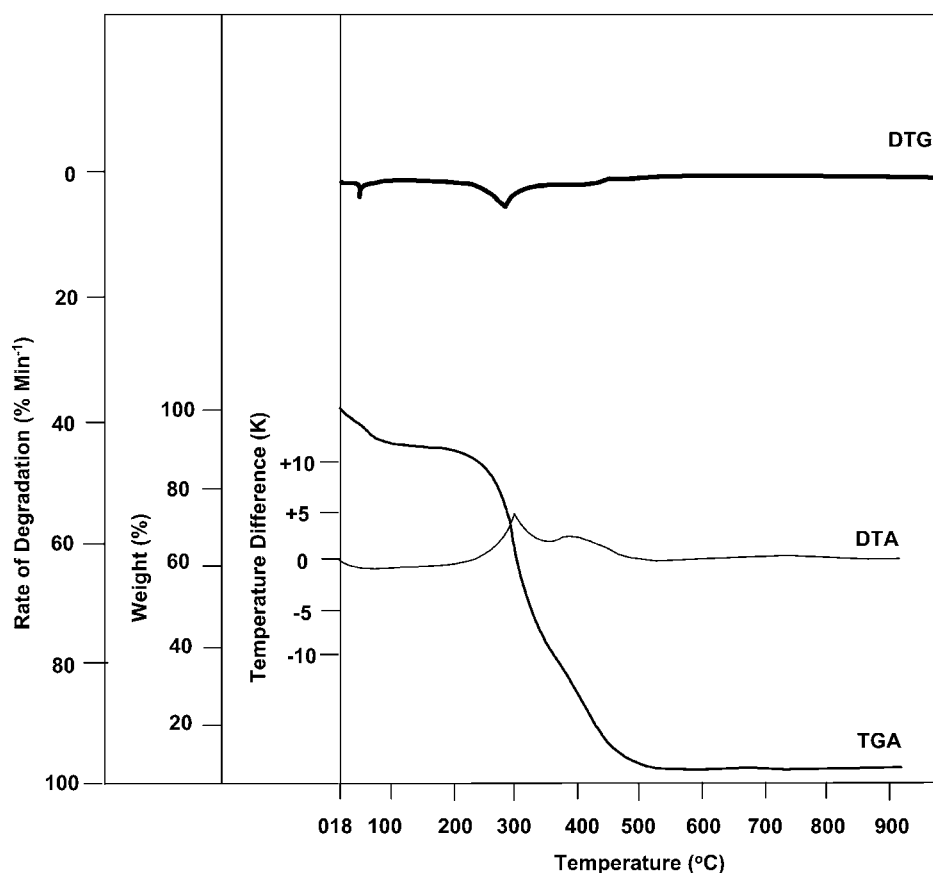


Fig. 1. Thermal degradation of pine needles in air (heating rate: 5 K min^{-1} ; air flow rate: 50 ml min^{-1}).

and thermal degradation characteristics at different heating rates. From Table 2 an irregular pattern in the distribution of volatiles evolved in different temperature ranges is found. The weight loss of the initial samples by the emanation of the volatiles in the temperature ranges of: (a) $200\text{--}280^\circ\text{C}$, (b) $280\text{--}320^\circ\text{C}$, (c) $320\text{--}500^\circ\text{C}$, and (d) $>500^\circ\text{C}$ is also reported in Table 2.

The total percentage of all the volatiles till the termination of volatilization process based on the original biomass weight (including moisture) and the PTFV (as a percentage of total volatile matter including moisture) are reported in Table 3. It is found that for pine needles it has a range of 46.5–67% of potential tar forming volatiles (PTFV), the fraction showing increasing trend as the heating rate increases. Increase in the heating rate reduces the residence time thus

accelerating the evolution of uncracked gases. DTG curves show consistently larger peaks as the heating rate is accelerated. This is manifested in the enhancement in the rate of maximum volatilization. These characteristics are compiled in Table 3 for different heating rates. As the heating rate increases, the maximum rate of volatilization, as represented by different TGA peak temperatures also goes up from 4.48 to 63.70% as the heating rate is accelerated from 5 to 30 K min^{-1} . The moisture is removed in the temperature range of $25\text{--}181^\circ\text{C}$ and the maximum rate of drying is in the range of 3.30–4.67% (weight loss per minute). Heating rate has tremendous influence on the thermal degradation characteristics of biomass components. The DTG curves show compartmental decomposition characteristics. The shorter small peak of volatilization at lower temperature

Table 2
Distribution of volatiles released during thermal degradation of pine needles in air

| Heating rate (K min^{-1}) | Weight loss (%) | | | | | Total volatile matter including moisture (%) | PTFV as percentage of total volatiles released at $320\text{--}500^\circ\text{C}$ |
|---|----------------------|---------------------------------|---------------------------------|---------------------------------|----------------------|---|--|
| | $<200^\circ\text{C}$ | $200\text{--}280^\circ\text{C}$ | $280\text{--}320^\circ\text{C}$ | $320\text{--}500^\circ\text{C}$ | $>500^\circ\text{C}$ | | |
| 5 | 10.71 | 13.78 | 26.02 | 46.50 | 2.04 | 98.00 | 46.50 |
| 10 | 9.58 | 10.21 | 19.79 | 56.46 | 3.96 | 96.00 | 54.20 |
| 15 | 9.69 | 6.63 | 13.27 | 66.33 | 4.08 | 98.00 | 65.00 |
| 25 | 9.38 | 5.21 | 13.54 | 67.70 | 4.17 | 96.00 | 65.00 |
| 30 | 8.51 | 4.25 | 12.77 | 71.28 | 3.19 | 94.00 | 67.00 |

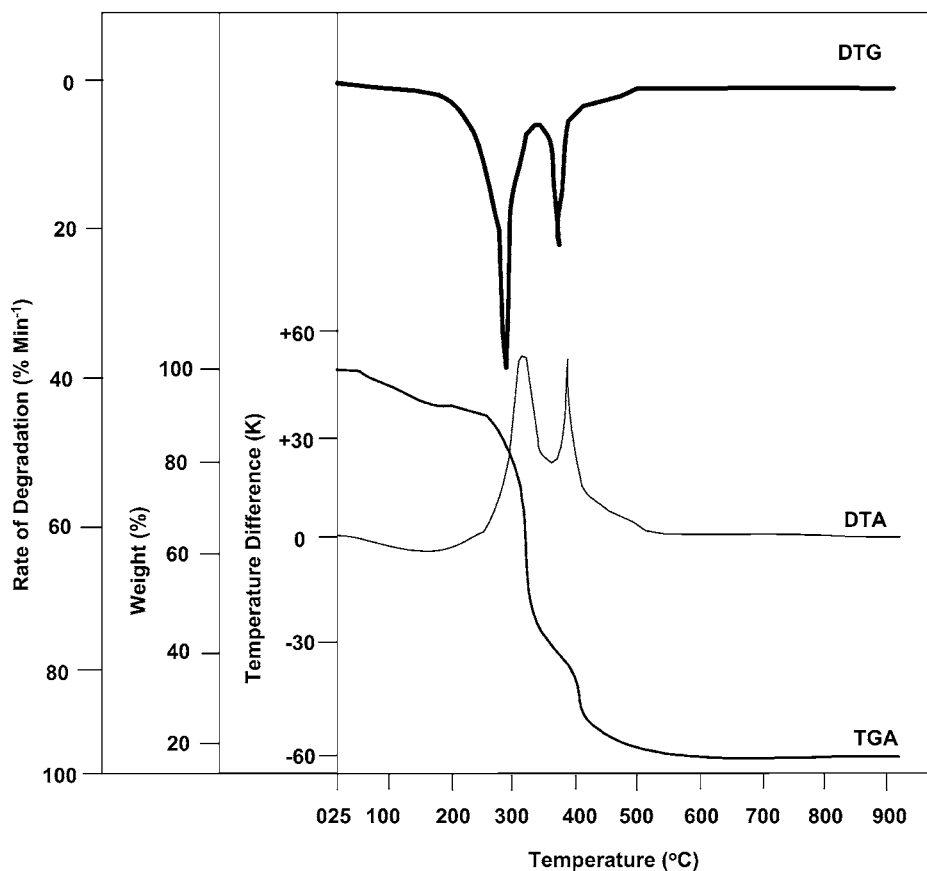


Fig. 2. Thermal degradation of pine needles in air (heating rate: 15 K min^{-1} ; air flow rate: 50 ml min^{-1}).

shows the decomposition of hemicellulose, while the larger peak at higher temperature shows the degradation of cellulose. The third peak shows the degradation of char. Lignin degrades throughout the temperature range. Heating rate also influences the heat absorption (endothermicity) and heat evolution (exothermicity) characteristics of the thermal degradation as seen from the DTA curves. It may be seen that the

entire degradation range may be divided in four degradation zones as found from the natural breaks in the slope of the TGA curves. The onset temperature of volatilization was found to be $181 \text{ }^\circ\text{C}$ at the heating rates of $15\text{--}30 \text{ K min}^{-1}$. The temperatures of maximum volatilization rate, as obtained from DTG peaks, were in the range of $248\text{--}310 \text{ }^\circ\text{C}$ ($T_{1 \text{ max}}$), of $290\text{--}395 \text{ }^\circ\text{C}$ ($T_{2 \text{ max}}$) and $310\text{--}484 \text{ }^\circ\text{C}$ ($T_{3 \text{ max}}$).

Table 3
Thermal degradation characteristics of pine needles in air

| Characteristics | Heating rate (K min^{-1}) | | | | |
|---|--------------------------------------|--------|--------|--------|--------|
| | 5 | 10 | 15 | 25 | 30 |
| Drying characteristics | | | | | |
| Drying range ($^\circ\text{C}$) | 27–107 | 25–130 | 27–157 | 28–142 | 51–181 |
| Moisture removed (%) | 8.00 | 8.00 | 9.10 | 8.00 | 8.00 |
| Maximum rate of drying ($\text{wt.}\% \text{ loss min}^{-1}$) | 3.48 | 4.67 | 3.52 | 3.30 | 3.50 |
| Pyrolysis characteristics | | | | | |
| Temperature of initial degradation | 192 | 192 | 181 | 181 | 181 |
| $T_{1 \text{ max}}$ ($^\circ\text{C}$) | 248 | 298 | 290 | 314 | 310 |
| $T_{2 \text{ max}}$ ($^\circ\text{C}$) | 290 | 395 | 390 | 375 | 370 |
| $T_{3 \text{ max}}$ ($^\circ\text{C}$) | 310 | 484 | 428 | 428 | 447 |
| T_c ($^\circ\text{C}$) | 438 | 503 | 508 | 526 | 575 |
| Maximum rate of volatilization | | | | | |
| $\text{wt.}\% \text{ min}^{-1}$ | 4.48 | 32.00 | 42.60 | 50.70 | 63.70 |
| $\text{wt.}\% \text{ }^\circ\text{C}^{-1}$ | 0.90 | 3.20 | 2.84 | 2.03 | 2.12 |

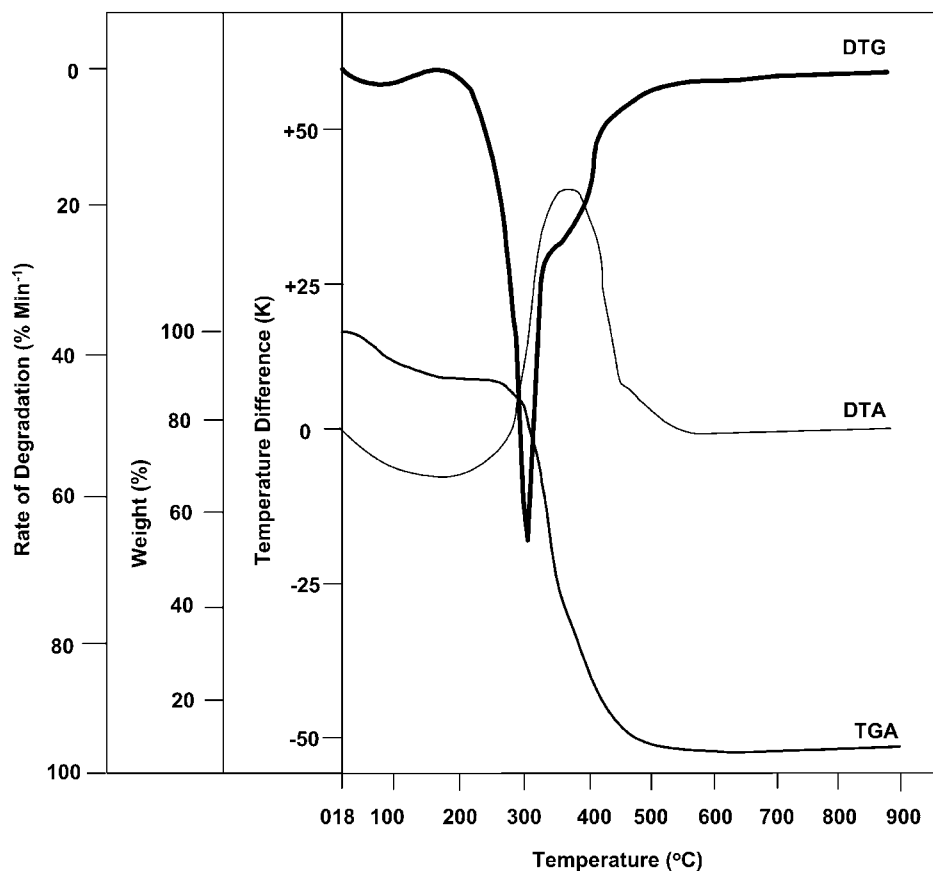


Fig. 3. Thermal degradation of pine needles in air (heating rate: 30 K min⁻¹; air flow rate: 50 ml min⁻¹).

The peak temperatures and the temperature difference (ΔT) values as obtained from the DTA curves are reported in Table 4. The transition temperatures (T_i) between endothermic drying (and probably the light volatiles evolution) and the exothermic degradation in air are listed for heating rates. The transition and the final temperature of degradation show upward trend with increase in the heating rate. It was found that the reaction was endothermic initially (due to drying and light volatile evolution) and thereafter it became exothermic. The first peak in DTA curves is probably due to the oxidation of volatiles, while the second peak probably represents the oxidation of charred residue. TG and DTG

curves are used in the determination of kinetic parameters for degradation of pine needles in air environment.

With the assumption that the biomass sample undergoes thermal degradation under oxidizing environment in any particular but clearly defined temperature zone as a single step, irreversible reaction and that the reaction velocity constant is represented by the Arrhenius equation i.e. $k = A \exp(-E/RT)$, the reaction rate, in terms of biomass fractional conversion, x , can be written as

$$\frac{dx}{dt} = A \exp\left(-\frac{E}{RT}\right) \phi(x) \quad (1)$$

Table 4

DTA data for thermal degradation of pine needles air flow rate: 50 ml min^{-1a}

| Heating rate (K min ⁻¹) | ΔT^b (K) | T_{P1} (K) | ΔT_1 (K) | T_{P2} (K) | ΔT_2 (K) | T_{P3} (K) | ΔT_3 (K) | T_e (K) | T_f (K) | T_t (K) |
|-------------------------------------|------------------|--------------|------------------|--------------|------------------|--------------|------------------|-----------|-----------|-----------|
| 5 | -2.38 | 305 | 10.2 | 394 | 4.42 | - | - | 243 | 449 | 346 |
| 10 | -3.3 | 331 | 31 | 399 | 12 | - | - | 248 | 505 | 354 |
| 15 | -4.76 | 331 | 36 | 399 | 36 | 490 | 3 | 248 | 517 | 375 |
| 25 | -8.6 | 395 | 44.9 | 433 | 33.7 | 466 | 6.7 | 269 | 526 | - |
| 30 | -9.2 | 409 | 45.5 | 456 | 35.6 | 475 | 7.9 | 271 | 535 | - |

^a Δ values refer to the difference in temperature due to exothermic reactions obtained at the peak temperature, T_P ; 1, 2, 3 refer to number of peaks observed in DTA curve; T_e refers to onset temperature of exothermic reaction; T_t refers to the transition temperature between endothermic drying and onset of exothermicity; T_f refers to the final temperature of exothermicity.

^b Drying.

Table 5
Determination of kinetic parameters by using different methods^a

| Method of analysis | The equations of determination of the kinetic parameters |
|---------------------------------|--|
| Coats and Redfern [5] | $\ln \left[\frac{-\ln(1-x)}{T^2} \right] = \ln \left[\frac{AR}{\beta E} \left(1 - \frac{2RT}{E} \right) \right] - \frac{E}{RT} \quad \text{for } n = 1.0,$ $\ln \left[\frac{-\ln\{1 - (1-x)^{1-n}\}}{(1-n)T^2} \right] = \ln \left[\frac{AR}{\beta E} \left(1 - \frac{2RT}{E} \right) \right] - \frac{E}{RT} \quad \text{for } n \neq 1.0$ |
| Agrawal and Sivasubramanian [6] | $\ln \left[\frac{-\ln(1-x)}{T^2} \right] = \ln \left[\frac{AR}{\beta E} \left(\frac{1-2(RT/E)}{1-5(RT/E)^2} \right) \right] - \frac{E}{RT} \quad \text{for } n = 1.0,$ $\ln \left[\frac{-\ln\{1 - (1-x)^{1-n}\}}{(1-n)T^2} \right] = \ln \left[\frac{AR}{\beta E} \left(\frac{1-2(RT/E)}{1-5(RT/E)^2} \right) \right] - \frac{E}{RT} \quad \text{for } n \neq 1.0$ |
| Freeman and Carroll [7] | $\frac{\Delta \log(\beta dx/dT)}{\Delta \log(1-x)} = n - \frac{E}{2.303R} \frac{\Delta(1/T)}{\Delta \log(1-x)}$ |
| Piloyan and Novikova [8] | $\ln \left(\frac{\omega}{T^2} \right) = \ln \frac{AR}{\beta E} - \frac{E}{RT}$ |
| Horowitz and Metzger [10] | $\ln[-\ln(1-\omega)] = \frac{E}{RT_p^2} \quad \text{when } n = 1, \quad \ln \left[\frac{1 - (1-\omega)^{1-n}}{1-n} \right] = \frac{E\theta}{RT_p^2} \quad \text{when } n \neq 1,$ <p>where $\theta = T - T_p$, T_p is the peak temperature as taken from the DTG curve</p> |
| Reich and Stivala [17] | $\ln \left[\frac{1 - (1-\omega_i)^{1-n}}{1 - (1-\omega_{i+1})^{1+n}} \left(\frac{T_{i+1}}{T_i} \right)^2 \right] = -\frac{E}{R} \left(\frac{1}{T_i} - \frac{1}{T_{i+1}} \right)$ |

^a ω is the decomposed fraction of solid at time t ; $W_r = W_\infty - W_t$ (mg); W_t the weight of biomass at any time (mg); W the weight of biomass at the completion of degradation (mg); $x = (W_0 - W_t)/(W_0 - W_\infty)$, fractional conversion; A the preexponential factor in the Arrhenius equation ($\text{mg}^{1-n} \text{min}^{-1}$); E the activation energy (kJ kg^{-1}); R the universal gas constant (kJ mol^{-1}); n the order of degradation reaction.

where A is the Arrhenius preexponential (or frequency) factor, E the activation energy, R the universal gas constant, T the absolute temperature, and $\phi(x)$ the function of x depending upon the reaction mechanism. Eq. (1) can be combined with the linear constant heating rate, $\beta = dT/dt$ to obtain the following equation:

$$\frac{dx}{dT} = \frac{A}{\beta} \exp \left(-\frac{E}{RT} \right) \phi(x) \quad (2)$$

and

$$f(x) = \int \frac{dx}{\phi(x)} = \frac{A}{\beta} \int_{T_0}^T \exp \left(-\frac{E}{RT} \right) dT \quad (3)$$

The first integral of Eq. (3) gives

$$f(x) = \ln \left[\frac{-\ln(1-x)}{T^2} \right], \quad n = 1.00 \quad (4)$$

and

$$f(x) = \ln \left[\frac{\ln\{1 - (1-x)^{1-n}\}}{(1-n)T^2} \right], \quad n \neq 1.00 \quad (5)$$

The symbols x , A , E , R and n are defined in Table 5.

Coats and Redfern [5] have initially suggested an approximation to the exponential integral which has been improved by Agrawal and Sivasubramanian [6]. Besides the integral expression as given by the above equations, differential method of Freeman and Carroll [7] and other methods are given in Table 5.

Table 6 presents the kinetic parameters, n , E and A for all the reaction (degradation) zones at different heating rates

using the integral method of Agrawal and Sivasubramanian [6]. The values of n reported in this table are the best fit values having the highest correlation coefficient, R^2 . The analysis of TGA data shows that the values of activation energy, E , and frequency factor, A , increase with increasing n .

Although the methods of Coats and Redfern [5], Agrawal and Sivasubramanian [6], Freeman and Carroll [7], Piloyan and Novikova [8] and Horowitz and Metzger [10] were also used for the determination of kinetic parameters, only the results of the integral method of Agrawal and Sivasubramanian [6] are presented in Table 6. The integral method has also been used by many investigators [2,3,13–15].

The values of E , A and n are obtained by the method of Agrawal and Sivasubramanian [6], by fitting the weight loss with temperature data for the entire temperature range. The activation energies and the preexponential factors are in the ranges of 30–250 kJ/mol and 10^2 to $>10^{21} \text{min}^{-1}$, respectively. These values are in the range of values reported by other investigators for various biomass materials and their components [4,9–12]. In the thermal degradation of pine needles in air, in general, the second, third and fourth zones of degradation show the largest values of activation energy while the overall activation energy is the lowest in comparison to the values obtained in various zones. However, it should be noted that the comparison of this nature has no meaning as the values are the best fit values at different orders of reaction.

Using Coats and Redfern [5] and Agrawal and Sivasubramanian [6] methods, it was observed that the initial

Table 6

Kinetic parameters of thermal degradation of pine needles in air heating rates: 5, 10, 15, 25 and 30 K min⁻¹ using Agrawal and Sivasubramanian method [6]^a

| Kinetic parameters | Heating rate (K min ⁻¹) | | | | |
|----------------------------------|-------------------------------------|-------------------------|-------------------------|-------------------------|-------------------------|
| | 5 | 10 | 15 | 25 | 30 |
| First reaction zone | | | | | |
| <i>n</i> | 0.50 | 1.00 | 0.00 | 2.50 | 2.00 |
| <i>E</i> (kJ mol ⁻¹) | 98.46 | 55.59 | 57.88 | 103.22 | 475.65 |
| <i>A</i> | 1.69 × 10 ⁵ | 2.95 × 10 ³ | 1.54 × 10 ⁵ | 7.58 × 10 ¹⁰ | 6.75 × 10 ⁴⁸ |
| <i>R</i> ² | 0.9857 | 0.9875 | 0.9938 | 0.9857 | 0.9978 |
| Second reaction zone | | | | | |
| <i>n</i> | 0.75 | 2.50 | 1.25 | 2.25 | 0.00 |
| <i>E</i> (kJ mol ⁻¹) | 144.79 | 414.66 | 110.62 | 131.19 | 61.61 |
| <i>A</i> | 2.40 × 10 ¹² | 1.53 × 10 ³⁴ | 1.56 × 10 ¹⁰ | 2.39 × 10 ¹¹ | 5.47 × 10 ⁴ |
| <i>R</i> ² | 0.9935 | 0.9876 | 0.9993 | 0.9956 | 0.9930 |
| Third reaction zone | | | | | |
| <i>n</i> | 2.25 | 2.50 | 2.50 | 1.75 | 2.50 |
| <i>E</i> (kJ mol ⁻¹) | 120.61 | 345.95 | 296.55 | 226.58 | 255.80 |
| <i>A</i> | 8.69 × 10 ⁸ | 7.35 × 10 ²⁵ | 6.06 × 10 ²³ | 2.48 × 10 ¹⁷ | 1.63 × 10 ¹⁹ |
| <i>R</i> ² | 0.9935 | 0.9358 | 0.9158 | 0.9995 | 0.9438 |
| Fourth reaction zone | | | | | |
| <i>n</i> | – | 2.50 | 1.75 | 2.50 | 2.50 |
| <i>E</i> (kJ mol ⁻¹) | – | 103.95 | 161.20 | 238.49 | 262.57 |
| <i>A</i> | – | 1.20 × 10 ⁶ | 7.25 × 10 ¹¹ | 5.40 × 10 ¹⁶ | 7.96 × 10 ¹⁷ |
| <i>R</i> ² | – | 0.9938 | 0.9583 | 0.9538 | 0.9367 |
| Entire reaction zone | | | | | |
| <i>n</i> | 1.00 | 2.50 | 1.25 | 1.50 | 2.50 |
| <i>E</i> (kJ mol ⁻¹) | 69.88 | 85.34 | 65.32 | 62.00 | 87.28 |
| <i>A</i> | 1.27 × 10 ⁵ | 5.98 × 10 ⁶ | 6.40 × 10 ⁴ | 4.52 × 10 ⁴ | 1.10 × 10 ⁷ |
| <i>R</i> ² | 0.9823 | 0.9632 | 0.9986 | 0.9928 | 0.9937 |

^a *A* has the dimension of min⁻¹ for *n* = 1 and mg^{1-*n*} min⁻¹ for any other value of *n*.

and final temperatures of active thermal degradation in air significantly affect the results from the two kinetic models. However, the methods of Coats and Redfern [5] and Agrawal and Sivasubramanian [6] gave same values of *E* at any best fit *n* value by using the linear least square method for the regression of the data. Freeman and Carroll [7] method has an advantage as it gives the kinetic parameters in one single step. However, the double differential of the experimental data increased the error in computation. The integral method with the approximation of Agrawal and Sivasubramanian [6] was found to be of immense use as the kinetic parameters obtained were the optimum values.

4. Conclusions

Thermal degradation of pine needles under oxidizing atmosphere at different heating rates as carried out in a Stanton Redcroft TG apparatus showed four distinct degradation zones. The second, third and fourth zone showed the fast degradations and gave highest values of activation energy. The kinetic parameters were determined by using Agrawal and Sivasubramanian [6] and other methods. How-

ever, Agrawal and Sivasubramanian [6] method was found to be most consistent. Excellent agreement between the experimental data and the model predictions were found. The relative simplicity of the Agrawal and Sivasubramanian [6] model gives it the potential for applications in the design of large scale biomass-thermal gasification units in the remote areas. The results of the least square regression showed that the kinetic parameters of pine needles at 30 K min⁻¹ heating rate of the total degradation zone has 96.67% confidence for the value of activation energy and the regression coefficient was 0.96.

References

- [1] M.J. Safi, M.Tech.(Chem.) Dissertation, Department of Chemical Engineering, Indian Institute of Technology, Roorkee, 2002.
- [2] P.V.R. Iyer, T.R. Rao, P.D. Grover, N.P. Singh, Thermochemical Characteristics of Biomass, Department of Chemical Engineering, IIT, Delhi, 1997.
- [3] P.B. Gangavati, Ph.D. Thesis, Department of Chemical Engineering, Indian Institute of Technology, Roorkee, 2002.
- [4] A.E. Ghaly, A. Ergudenler, A.M. Al Taweel, Biomass Bioenergy 6 (1993) 457.
- [5] A.W. Coats, J.P. Redfern, Nature 201 (1964) 68.
- [6] R.K. Agarwal, M.S. Sivasubramanian, AIChE J. 33 (1987) 7.

- [7] E.S. Freeman, B. Carroll, *J. Phys. Chem.* 62 (1958) 394.
[8] G.O. Piloyan, O.S. Novikova, *J. Inorg. Chem.* 12 (1967) 313.
[9] C.-H. Li, *AIChE J.* 31 (1985) 6.
[10] H.H. Horowitz, G. Metzger, *Anal. Chem.* 35 (1963) 1464.
[11] K.G. Mansaray, A.E. Ghaly, *Energy Sources* 21 (1999) 899.
[12] M.N. Mamdouh, *Wood Fiber Sci.* 17 (1985) 266.
[13] A.K. Jain, S.K. Sharma, D. Singh, *J. Solar Energy Eng. (ASME)* 121 (5) (1999) 25.
[14] S.K. Katyal, *Ind. Chem. Eng. A* 43 (1) (2001) T20.
[15] S.K. Katyal, P.V.R. Iyer, *Energy Sources* 22 (2000) 363.
[16] V.R.K. Prasad, J.L. Kuester, *Ind. Eng. Chem. Res.* 27 (1988) 304.
[17] L. Reich, S.S. Stivala, *Thermochim. Acta* 24 (1980) 9.